

Observation and Interpretation of Annulated Porphyrins: Studies on the Photophysical Properties of *meso*-Tetraphenylmetalporphyrins

Joy E. Rogers,^{*,†,‡} Kiet A. Nguyen,^{*,†,‡} David C. Hufnagle,^{†,§} Daniel G. McLean,^{†,⊥} Weijie Su,^{†,§} Kristi M. Gossett,^{†,§} Aaron R. Burke,^{†,§} Sergei A. Vinogradov,[#] Ruth Pachter,[†] and Paul A. Fleitz[†]

Materials and Manufacturing Directorate, Air Force Research Laboratory, MLPJ, 3005 Hobson Way Bldg 651, Wright Patterson Air Force Base, Ohio 45433; UES, Inc., Dayton, Ohio 45432; Anteon Corporation, Dayton, Ohio 45431; Science Applications International Corporation, Dayton, Ohio 45434; and Department of Biochemistry and Biophysics, University of Pennsylvania, Philadelphia, Pennsylvania 19104

Received: May 27, 2003; In Final Form: August 4, 2003

We present results of a joint computational and experimental study for a series of annulated metalloporphyrins in order to establish structure–property relationships. Specifically, we have examined the effects of substitution by *meso*-tetraphenylation, tetrabenzoyl and tetranaphthoyl annulation, and effects of changing the central metal from zinc (Zn) to palladium (Pd). Utilizing absorption and emission spectroscopy and laser flash photolysis techniques, the photophysical properties of these porphyrins have been determined. Upon the addition of benzo or naphtho groups, we observed an overall red shift in the ground state absorption spectra of both the B-bands and the Q-bands with increased conjugation and an increase in the Q-band to B-band intensity ratios. Time-dependent density functional theory calculations were performed on both series of porphyrins to identify the effects of phenyl, benzo, and naphtho substituents on the spectra. The benzo and naphtho adducts provide a larger contribution (typically 40–90%) to the observed red shifts due to increased π -conjugation, while there is a smaller contribution (typically 0–25%) from distortion of the porphyrin. Similarly, a red shift for the T_1 – T_n absorption spectrum and an overall general broadening in the spectrum were found with increased conjugation. An increase in the triplet molar extinction coefficient through the near-infrared region with annulation was also found. Varying the metal has an effect on the overall absorption spectra; i.e., the ground state spectra of the Zn porphyrins are red-shifted relative to the Pd porphyrins. For the triplet excited state spectra there were small effects in the spectra by changing the metal with a significant contribution to the kinetic properties by the heavy atom effect of the Pd.

Introduction

Porphyrins form an important class of chromophores that are being developed and used for many different applications such as photodynamic therapy, commercial dye industry, nonlinear absorption, artificial photosynthesis, oxygen transport, and solar energy conversion.¹ Much research has been done to develop new porphyrin chromophores that display certain characteristics dependent on the application of use.² The understanding of structure–property relationships is crucial for the development of novel porphyrins targeted for specific applications. In the work presented here we focus on the structure–property relationships in a series of *meso*-tetraphenylporphyrins that have been modified by annulation of the pyrrole ring with either benzo or naphtho substituents.

The metalated *meso*-tetraphenyltetrabenzoporphyrin (MTPTBP) and *meso*-tetraphenyl[2,3]tetranaphthoporphyrin (MTPTNP) shown in Figure 1 were previously synthesized,^{3–13} but relatively few thorough and comprehensive studies were carried out. Several papers have been published in which MTPTBP and

MTPTNP are studied and compared with similar systems that do not contain the *meso*-phenyl groups, i.e., tetrabenzoporphyrin (MTBP) and tetranaphthoporphyrin (MTNP). The qualitative observations, e.g., red shifts in the ground and excited state spectra with annulation, are discussed, but no attempt to quantify the data was made.^{11–16} We synthesized the same series of chromophores and report a detailed quantitative study of photophysical parameters. In addition, calculations using time-dependent density functional theory (TDDFT) were carried out to interpret the observed spectra and to shed light on the origin of the spectral shifts.

Experimental Section

Synthesis. ZnP and PdP were both purchased from Frontier Scientific, Inc., with 97% purity and used as received.

ZnTPP. Chlorin-free ZnTPP was purchased from Frontier Scientific, Inc., with 97% purity and used as received.

ZnTPTBP. In the preparation of ZnTPTBP the template method, developed by Kopranev et al.¹¹ and improved by Ichimura et al.,¹⁷ was utilized. A mixture of phthalimide, zinc benzoate, and phenylacetic acid (with molar ratio 1:1:2) was well ground together and put into a 25 mL flask and heated at 360–380 °C for 1 h under a N₂ atmosphere. After the reaction mixture was cooled and washed with hot water several times, the reaction product was extracted with chloroform and purified

[†] Air Force Research Laboratory.

[‡] UES, Inc.

[§] Anteon Corporation.

[⊥] Science Applications International Corporation.

[#] University of Pennsylvania.

* Corresponding author: E-mail: Joy.Rogers@wpafb.af.mil (exp.), Kiet.Nguyen@wpafb.af.mil (theoret.).

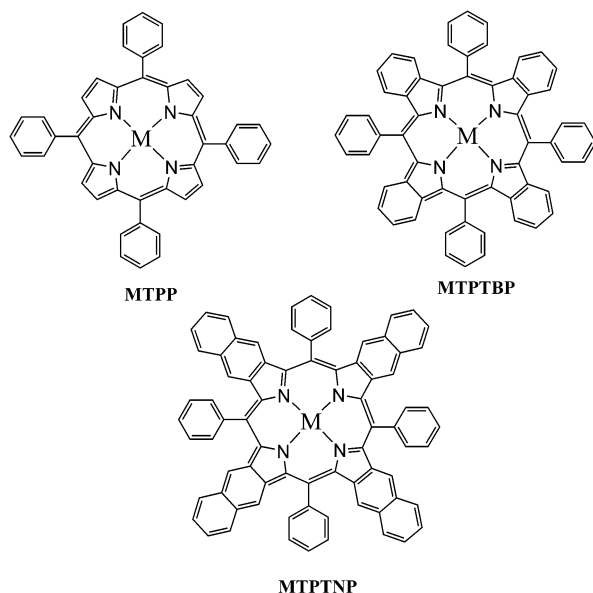


Figure 1. Shown are the structures of the porphyrin series MTTP (*meso*-tetraphenylporphyrin), MTPTBP (*meso*-tetraphenyltetrabenzoporphyrin), and MTPTNP (*meso*-tetraphenyltetranaphthoporphyrin). The metal (M) is either Pd or Zn.

by repeated chromatography on a column of aluminum oxide using benzene/hexanes/THF (10:10:1). Thin-layer chromatography, UV/vis absorption, and NMR were used to check the purity of the sample. ^1H NMR (CDCl_3 , 300 MHz): 8.30 (d, 8H, ortho phenyl), 7.95 (t, 4H, para phenyl), 7.87 (t, 8H, meta phenyl), 7.28 (dd, 8H, B position on benzo ring), 7.17 (dd, 8H, A position on benzo ring). The NMR spectrum matches that obtained by Ichimura et al.,³ Cheng et al.,⁴ and Ito et al.⁹

ZnTPTNP. This synthesis followed the template method by Kopranev et al.¹³ A mixture of 2,3-naphthalenecarboximide, zinc benzoate, and phenylacetic acid (with molar ratio 1:1:2) was used. The reaction product was purified by repeated chromatography with chloroform first and then with chloroform/hexanes/THF (30:10:1) on a column of neutral aluminum oxide. Thin-layer chromatography, UV/vis absorption, and NMR were used to check the purity of the sample. Because of the instability of the compound, the sample may contain contaminants of degraded or otherwise changed material. ^1H NMR (CDCl_3 , 300 MHz): 8.41 (d, 8H, ortho phenyl), 8.10 (t, 4H, para phenyl), 7.97 (t, 8H, meta phenyl), 7.69 (m, 16H, B and C positions on naphtho rings), 7.45 (m, 8H, A position on naphtho rings). The NMR data matched that obtained by Ito et al.¹⁰

PdTPP. PdTPP (97%) was purchased from Frontier Scientific, Inc., and used as received.

PdTPTBP. The synthesis of PdTPTBP was done according to the previously published procedure.⁷ ^1H NMR (CDCl_3 , 300 MHz): 8.27 (d, 8H, ortho phenyl), 7.91 (d, 4H, para phenyl), 7.86 (d, 8H, meta phenyl), 7.21 (m, 8H, B position on benzo ring), 7.11 (m, 8H, A position on benzo ring).

PdTPTNP. This compound was synthesized as previously reported.^{18,19} ^1H NMR ($\text{DMF-}d_7$, 500 MHz): 8.38 (8H, ortho phenyl), 8.22 (4H, para phenyl), 8.09 (8H, meta phenyl), 7.66 (16H, B and C positions on naphtho rings), 7.57 (8H, A position on naphtho rings).

General Techniques. Ground state UV/vis absorption spectra were measured on a Cary 500 spectrophotometer in air-saturated pyridine. Emission spectra were measured using a Perkin-Elmer model LS 50B fluorometer or a Spex Fluorolog-2 using an IR-sensitive PMT (Hamamatsu R2658P). Oxygen was removed from the sample for the room temperature fluorescence and

phosphorescence measurements by either bubbling with argon or by three successive freeze–pump–thaw cycles. Nanosecond transient absorption measurements were carried out in deoxygenated pyridine (by three successive freeze–pump–thaw cycles) using the third harmonic (355 nm) of a Q-switched Nd:YAG laser (Continuum YG661, pulse width ca. 15 ns). Pulse fluences of up to 8 mJ cm^{-2} at the excitation wavelength were typically used. A detailed description of the laser flash photolysis apparatus has been given earlier.²⁰

Fluorescence quantum yields were determined using the actinometry method previously described.²⁰ Zinc *meso*-tetraphenylporphyrin was used as an actinometer with a known fluorescence quantum yield of 0.033 in deaerated benzene.²¹ All samples were deoxygenated using the freeze–pump–thaw method and excited at 500 nm with a matched optical density of 0.1. Phosphorescence quantum yields and time-resolved measurements were done as previously described.¹⁹

The molar absorption coefficients of the porphyrin triplet states were determined in deoxygenated pyridine using the method of singlet depletion, which has been described previously.²⁰ Quantum yields for intersystem crossing of the Zn series were determined using the method of relative actinometry as previously described utilizing a benzophenone actinometer.²⁰ Matched optical densities of the porphyrins (deoxygenated pyridine) and benzophenone (air-saturated benzene) at 355 nm were utilized in each determination. For the Pd chromophores photoacoustic calorimetry was utilized to measure intersystem crossing quantum yields as previously reported.²²

Computational Studies. The calculations were carried out using TDDFT^{23–25} with Becke's three-parameter hybrid exchange-correlation functional (B3LYP)^{26–28} and the 6-31G(d)^{29,30} basis set for carbon, hydrogen, and nitrogen atoms and the effective core potentials (ECP) and basis sets of Stevens et al.^{31,32} for the central metals. The structures used in the TDDFT calculations have been predicted using the Kohn–Sham (KS)³³ density functional theory with the same ECP and basis sets as those used in the excited state calculations. These structures were verified to be minima with a smaller 6-31G basis set. All electronic structure calculations were carried out using the Gaussian 98 program.³⁴

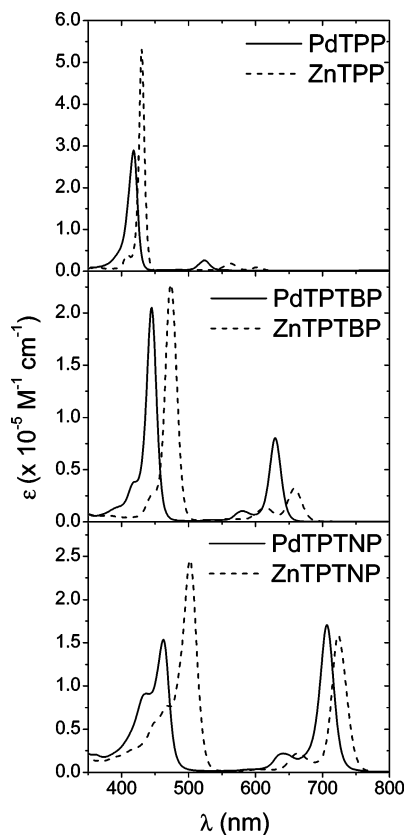
Results

In this work we are interested in establishing structure–property relationships by systematically studying a series of structurally related porphyrins to understand how chemical changes affect the photophysical properties. A series of porphyrins were synthesized with increased degree of conjugation of the macrocycle by addition of fused benzo or naphtho groups to the pyrrole ring. Shown in Figure 1 are the structures of the porphyrins (MTTP, MTPTBP, and MTPTNP); M denotes a metal, which is either Zn or Pd.

Ground State Absorbance. Shown in Figure 2 are the ground state spectra of both series of porphyrins in air-saturated pyridine. The molar extinction coefficients are given in Table 1 in both pyridine and benzene. These agree with literature data for various solvents.^{3,7,10,35,36} ZnTPTBP and ZnTPTNP are not stable in benzene when left in the room light so therefore we switched our solvent to pyridine where these chromophores are reasonably stable. We included the data in benzene because they show that there is a large red shift of the Zn series in pyridine with no shift in the Pd series. It is known that pyridine coordinates with the Zn by axial ligation,^{14,37,38} therefore stabilizing the chromophore by lowering the energy. It was observed in both solvents that annulation with the benzo or

TABLE 1: Ground State Absorption Data

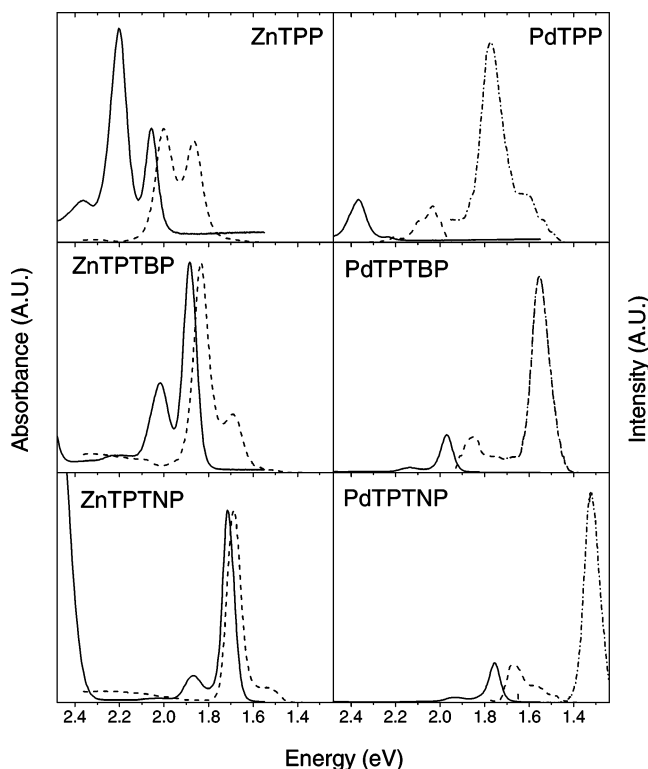
transition/solvent	ZnTPP	ZnTPTBP	ZnTPTNP	PdTPP	PdTPTBP	PdTPTNP
B-band						
benzene	423 nm (2.93 eV)	463 nm (2.68 eV)	482 nm (2.57 eV)	418 nm (2.97 eV)	444 nm (2.79 eV)	463 nm (2.68 eV)
ϵ ($\times 10^{-5}$) ($M^{-1} cm^{-1}$)	4.35 ± 0.03			2.81 ± 0.18	2.64 ± 0.03	1.44 ± 0.05
pyridine	431 nm (2.88 eV)	473 nm (2.62 eV)	502 nm (2.47 eV)	418 nm (2.97 eV)	444 nm (2.79 eV)	463 nm (2.68 eV)
ϵ ($\times 10^{-5}$) ($M^{-1} cm^{-1}$)	5.33 ± 0.51	2.21 ± 0.14	2.42 ± 0.09	2.90 ± 0.14	1.97 ± 0.24	1.55 ± 0.04
TDDFT	382 nm (3.25 eV)	422 nm (2.94 eV)	431 nm (2.88 eV)	382 nm (3.25 eV)	415 nm (2.99 eV)	423 nm (2.93 eV)
oscillator strength (f)	1.19	1.25	1.20	1.10	1.01	0.97
Q-band						
benzene	588 nm (2.11 eV)	653 nm (1.90 eV)	725 nm (1.71 eV)	551 nm (2.24 eV)	629 nm (1.97 eV)	705 nm (1.76 eV)
ϵ ($\times 10^{-5}$) ($M^{-1} cm^{-1}$)	0.03 ± 0.01			0.02 ± 0.01	1.05 ± 0.07	1.68 ± 0.08
pyridine	602 nm (2.06 eV)	660 nm (1.88 eV)	725 nm (1.71 eV)	554 nm (2.24 eV)	629 nm (1.97 eV)	709 nm (1.75 eV)
ϵ ($\times 10^{-5}$) ($M^{-1} cm^{-1}$)	0.10 ± 0.01	0.31 ± 0.02	1.57 ± 0.05	0.02 ± 0.01	0.80 ± 0.11	1.71 ± 0.05
TDDFT	539 nm (2.30 eV)	605 nm (2.05 eV)	681 nm (1.82 eV)	517 nm (2.40 eV)	579 nm (2.14 eV)	653 nm (1.90 eV)
oscillator strength (f)	0.02	0.09	0.28	0.01	0.12	0.31

**Figure 2.** Ground state absorption of MTPP, MTPTBP, and MTPTNP (M = Pd or Zn). Extinction coefficients are given for absorbance data. All data were obtained at room temperature (25 °C) in pyridine.

naphtho group results in red shifts of both the B-bands and the Q-bands, where the Q-bands gain intensity while the B-bands lose intensity (Table 1).

Fluorescence and Phosphorescence. Typical S_1-S_0 emission from both series of porphyrins is shown in Figure 3. The fluorescence quantum yields (Φ_f) were determined using zinc *meso*-tetraphenylporphyrin (ZnTPP) as a standard with a known quantum yield of 0.033 in deaerated benzene.²¹ These are given in Table 2 along with the singlet state energy (E_{S_1}). Fluorescence quantum yields in deoxygenated pyridine for ZnTPP and PdTPP are consistent with measurements in other solvents.³⁹

For the Pd series, room temperature phosphorescence was easily observed in the absence of oxygen, and it is shown in Figure 3. Room temperature phosphorescence was observed for ZnTPP and ZnTPTNP under argon in pyridine. Phosphorescence of ZnTPTBP at room temperature in deoxygenated pyridine was not observed. The phosphorescence quantum yields (Φ_p) at room

**Figure 3.** Q-band absorbance and emission of MTPP, MTPTBP, and MTPTNP (M = Pd or Zn). Extinction coefficients are given for absorbance data (left axis); all others are in intensity (arbitrary units, right axis). All data were obtained at room temperature (25 °C) in pyridine. Samples were excited at 500 nm.

temperature are reported in Table 2. Our work is consistent with other measurements of room temperature phosphorescence quantum yields for PdTPTBP,⁷ PdTPTNP,¹⁹ and ZnTPTNP¹⁹ in DMF.

T_1-T_n Properties. Figure 4 shows the transient observed upon 355 nm excitation of each of the porphyrins in deoxygenated pyridine. The identities of the transients were confirmed by molecular oxygen quenching of the excited state. The T_1-T_n molar extinction coefficients were determined using a singlet depletion method. The values determined are ZnTPP $\epsilon_{475nm} = 76\,000 \pm 4000 M^{-1} cm^{-1}$, ZnTPTBP $\epsilon_{550nm} = 46\,000 \pm 2000 M^{-1} cm^{-1}$, ZnTPTNP $\epsilon_{475nm} = 58\,000 \pm 3000 M^{-1} cm^{-1}$; $\epsilon_{595nm} = 57\,000 \pm 3000 M^{-1} cm^{-1}$, PdTPP $\epsilon_{475nm} = 54\,000 \pm 3000 M^{-1} cm^{-1}$, PdTPTBP $\epsilon_{530nm} = 36\,000 \pm 2000 M^{-1} cm^{-1}$, and PdTPTNP $\epsilon_{480nm} = 45\,000 \pm 2000 M^{-1} cm^{-1}$; $\epsilon_{610nm} = 33\,000 \pm 2000 M^{-1} cm^{-1}$. Our data are consistent with values reported in the literature for ZnTPP,^{21,40} PdTPP,³⁵ and ZnTPTBP.^{41,42}

TABLE 2: Photophysical Properties of Porphyrins in Pyridine

	ZnTPP	ZnTPTBP	ZnTPTNP	PdTPP	PdTPTBP	PdTPTNP
Fl Q (0,0)	620 nm	676 nm	736 nm	565 nm	669 nm	741 nm
Φ_{fl}^a	0.029 ± 0.003	0.007 ± 0.001	0.052 ± 0.016	~ 0.0004	~ 0.0003	~ 0.0003
E_{S1} (eV) ^b	2.03	1.86	1.70	2.22	1.92	1.72
Ph λ_{max}	804 nm		972 nm	705 nm	797 nm	937 nm
Φ_p	0.0005 ± 0.0001	< 0.00001	0.0002 ± 0.0001	0.0040 ± 0.0003	0.167 ± 0.005	0.065 ± 0.002
E_{T1} (eV) ^c	1.58		1.29	1.82	1.59	1.36
ΔE_{S1T1} (eV)	0.45		0.41	0.40	0.33	0.36
T_1-T_n λ_{max}	475 nm	550 nm	475, 595 nm	475 nm	530 nm	480, 610 nm
Φ_{ISC}	0.84 ± 0.07	0.94 ± 0.08	0.62 ± 0.13	0.96 ± 0.04	0.97 ± 0.06	0.77 ± 0.07
τ_T (μs) ^d	> 406	148 ± 3	> 225	65 ± 3	143 ± 20	65 ± 10
τ_T (μs) ^e	3680	167	440	11	195	60

^a Oxygen removed from sample by three freeze–pump–thaw cycles. ^b Value obtained from cross section of red edge of absorbance and blue edge of fluorescence. ^c Value obtained from blue edge of phosphorescence. ^d Oxygen removed from sample by three freeze–pump–thaw cycles. Measured by laser flash photolysis. ^e Oxygen removed by bubbling with argon. Measured by phosphorescence decay at room temperature.

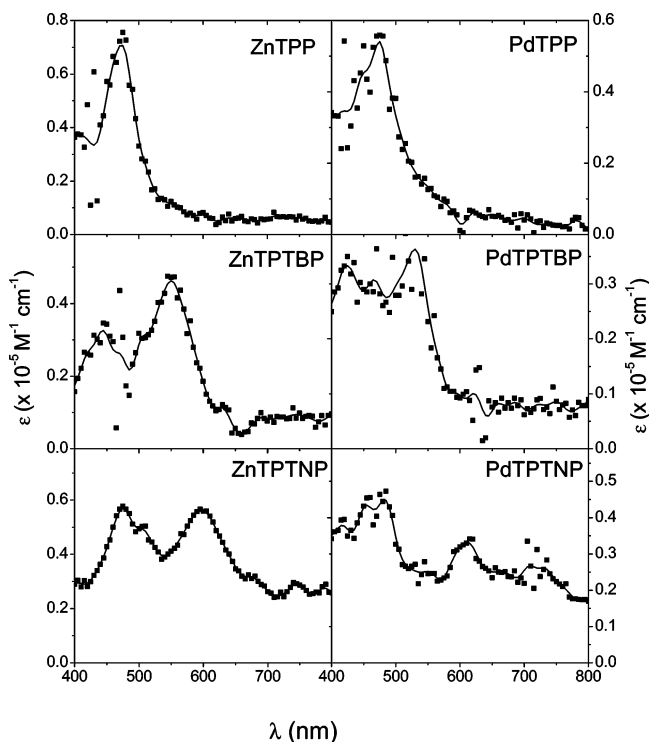


Figure 4. Triplet excited state absorbance data (T_1-T_n) observed after nanosecond pulsed 355 nm excitation of MTTP, MTPTBP, and MTPTNP ($M = Pd$ or Zn) in deoxygenated pyridine. Triplet excited state molar absorption coefficients were obtained using the method of singlet depletion as described in the text.

Shown in Table 2 are the triplet excited state lifetimes (τ_T) in deoxygenated pyridine. They were determined and are reported by both laser flash photolysis and time-resolved phosphorescence measurements. Using the laser flash photolysis experiment for PdTPP in pyridine, the data were fit to a first-order exponential decay with a lifetime of $65 \pm 3 \mu s$. However, the transient does not return to the baseline, indicating that a long-lived transient is formed. We did not observe this in benzene. This suggests that either the singlet excited state or the triplet excited state of PdTPP is reacting with the pyridine. Also reported in Table 2 are the intersystem crossing quantum yields (Φ_{ISC}). We observe that Φ_{ISC} is smaller for the MTPTNP chromophores than the others. The Φ_{ISC} for ZnTPP has been reported as 0.88 in benzene²¹ and for PdTPP 1.00 in ethanol.⁴³ Our values are within the error margins of these numbers.

Discussion

Porphyrins are an important class of materials and have attractive characteristics that make them widely used in various

fields of science and engineering.¹ The ability to simply change the central metal allows for variations in the overall properties and also provides some fine-tuning capabilities. In general, metalloporphyrins contain two types of metals: regular metals or irregular metals.⁴⁴ Regular metals, like Zn, have only a small effect on the optical absorption and emission spectra, which is understood as a small perturbation on the π electrons of the porphyrin ring. Irregular metals, e.g. Pd, have much stronger effects on absorption and emission of porphyrins, either through stronger mixing or through the introduction of new low-energy optical transitions. Varying the metal centers as well as changing the ring structure alters the photophysical properties of metalloporphyrins. It is interesting and important to understand how these changes affect the overall photophysical properties of the chromophores. We will discuss the effects of increasing the conjugation due to annulation of the porphyrin ring and also the effects of changing the central metal from Zn to Pd. We begin with the spectral changes observed and then discuss the kinetic properties.

Spectral Changes. Effect of Extension of Porphyrin Ring. Extension of the porphyrin ring by benzo and naphtho annulation results in red shifts in both the ground (Q- and B-bands) and triplet excited state (T_1-T_n) absorption spectra. It is known that red shifts of the ground state spectra may be attributed to some extent to saddling/ruffling of the porphyrin as well as electronic effects due to increased π -conjugation, a notion that is continuously being addressed with a range of substitutions.⁴⁵ To assess the relative contributions of distortion and increased π -conjugation, we compiled the experimental and theoretical results from model compounds not containing *meso*-phenyl substituents that directly compare the data from our series of chromophores. The model compounds are: unsubstituted Zn porphyrin (ZnP), Pd porphyrin (PdP), Zn tetrabenzoporphyrin (ZnTBP),⁴⁶ Pd tetrabenzoporphyrin (PdTBP),⁴⁶ Zn tetranaphthoporphyrin (ZnTNP),¹³ and Pd tetranaphthoporphyrin (PdTNP).¹⁸ These compounds are all planar in the ground state, which make them useful for understanding spectral red shifts that are due to purely electronic effects.

In Table 3 both the theoretical and experimental data are shown for the excitation energies of the B and the Q-bands of both the Zn and Pd series. The total red shift for a given band, relative to ZnP or PdP, is due to the additive effects of (a) the *meso*-phenyl groups, (b) the benzo groups (for MTPTBP), (c) the naphtho groups (for MTPTNP), (d) nonplanar distortion, (e) combined effects of nonplanar distortion, *meso*-tetraphenylolation and tetrabenzoannulation (for MTPTBP), and (f) combined effects of nonplanar distortion, *meso*-tetraphenylolation, and tetranaphthoannulation (for MTPTNP). The difference in energy relative to the planar Zn or Pd porphyrin is given in Table 3

TABLE 3: TD-B3LYP/6-31G(d) Excitation Energies (E in eV) for Zinc and Palladium Porphyrins (Experimental Data Measured in Pyridine)

system/transition	E (eV) theo (exp)	ΔE (eV)	system/transition	E (eV) theo (exp)	ΔE (eV)
ZnP (D_{4h})			PdP (D_{4h})		
1 ¹ E _u (Q)	2.44 (2.19)	0.00	1 ¹ E _u (Q)	2.54 (2.32)	0.00
2 ¹ E _u (B)	3.54 (3.05)	0.00	2 ¹ E _u (B)	3.49 (3.16)	0.00
ZnTPP (D_{4h}) ^a			PdTPP (D_{4h}) ^a		
1 ¹ E _u (Q)	2.35	0.09	1 ¹ E _u (Q)	2.45	0.09
2 ¹ E _u (B)	3.34	0.20	2 ¹ E _u (B)	3.31	0.18
ZnTBP (D_{4h})			PdTBP (D_{4h})		
1 ¹ E _u (Q)	2.18 (1.97) ^b	0.26 (0.22)	1 ¹ E _u (Q)	2.26 (2.04) ^b	0.28 (0.28)
3 ¹ E _u (B)	3.28 (2.88) ^b	0.26 (0.17)	2 ¹ E _u (B)	3.29 (3.05) ^b	0.20 (0.11)
ZnTNP (D_{4h})			PdTNP (D_{4h})		
1 ¹ E _u (Q)	1.90 (1.77) ^c	0.54 (0.42)	1 ¹ E _u (Q)	1.97 (1.77) ^d	0.57 (0.55)
3 ¹ E _u (B)	3.13 (2.82) ^c	0.41 (0.23)	3 ¹ E _u (B)	3.17 (2.81) ^d	0.32 (0.35)
ZnTPP (D_{2d})			PdTPP (D_{2d})		
1 ¹ E (Q)	2.30 (2.06)	0.14 (0.13)	1 ¹ E (Q)	2.40 (2.24)	0.14 (0.08)
2 ¹ E (B)	3.25 (2.88)	0.29 (0.17)	4 ¹ E (B)	3.25 (2.97)	0.24 (0.19)
ZnTPTBP (D_{2d})			PdTPTBP (D_{2d})		
1 ¹ E (Q)	2.05 (1.88)	0.39 (0.31)	1 ¹ E (Q)	2.14 (1.97)	0.40 (0.35)
2 ¹ E (B)	2.94 (2.62)	0.60 (0.43)	2 ¹ E (B)	2.99 (2.79)	0.50 (0.37)
ZnTPTNP (D_{2d})			PdTPTNP (D_{2d})		
1 ¹ E (Q)	1.82 (1.72)	0.62 (0.47)	1 ¹ E (Q)	1.90 (1.75)	0.64 (0.57)
2 ¹ E (B)	2.88 (2.47)	0.66 (0.58)	3 ¹ E (B)	2.93 (2.68)	0.56 (0.48)

^a The *meso*-phenyl groups constrained to a planar geometry. ^b *Opt. Spectrosc.* **1973**, *34*, 635. ^c In DMF; *J. Gen. Chem. USSR* **1985**, *55*, 803. ^d In DMF; *Adv. Exp. Med. Biol.* **1997**, *411*, 597.

TABLE 4: Contributions (All Values in %) to Red Shift in Ground State Absorption Spectrum (Experimental Data Measured in Pyridine)

	effect of phenylation	effect of benzo annulation ^c	effect of naphtho annulation ^d	total substituent effect	distortion ^e and other effects ^{f-h}
ZnTPTBP					
Q	23 ^a (42) ^b	67 (71)		90 (113)	10 (0)
B	33 (40)	43 (40)		76 (80)	24 (20)
ZnTPTNP					
Q	15 (28)		87 (89)	102 (117)	0 (0)
B	30 (29)		62 (40)	92 (69)	8 (31)
PdTPTBP					
Q	23 (23)	70 (80)		93 (103)	7 (0)
B	36 (51)	40 (30)		76 (81)	24 (19)
PdTPTNP					
Q	14 (14)		89 (96)	103 (110)	0 (0)
B	32 (40)		57 (73)	89 (113)	11 (0)

^a The *meso*-phenyl groups constrained to a planar conformation (theoretical data only). ^b The *meso*-phenyl groups (experimental data only). ^c The benzo groups. ^d The naphtho groups. ^e Nonplanar distortion. ^f Combined effects of nonplanar distortion, *meso*-tetraphenylation, and tetrabenzo annulation. ^g Combined effects of nonplanar distortion, *meso*-tetraphenylation, and tetranaphtho annulation. ^h Determined by subtracting the total substituent effect from 100.

(ΔE) for both the theoretical and experimental data. Analysis of the shifts suggests that geometry of distortion, which facilitates the interactions between the porphyrin extended macrocycle and *meso*-phenyls, plays a role in the observed red shift (Table 4). By comparing red shifts observed for the model systems with those of our porphyrins, it is possible to discern the overall contribution of each type of substitution in MTPTBP and MTPTNP. The percentage is determined by dividing the change in the energy (ΔE) of either the effect of phenylation, benzo annulation, or naphtho annulation by the change in the energy (ΔE) of all effects MTPTBP and MTPTNP. These percentages are given in Table 4 for the corresponding functional group contribution for both theoretical and experimental results.

The data show that a large percentage of the red shifts observed for MTPTBP and MTPTNP is due to electronic effects, which result from increased π -conjugation from the added benzo or naphtho groups. Comparing MTPTBP and MTPTNP, for both Zn and Pd, the effect of the addition of the four *meso*-phenyl groups (theoretical data) is approximately one-quarter of the total for the B-band and one-third of the total for the Q-band. A large contribution, more than 70% of the total for the Q-band and more than 40% of the total for the B-band, is attributed to

benzo and naphtho annulation. Thus, only about 25%–0% is attributed to geometrical distortion and any other contributing effects depending on the band and compound. There is a larger effect observed for the Q-band than the B-band with annulation. This is consistent with the origins of these transitions shown in Figures 5 and 6. Note that the HOMO (b_2) coefficients are largely localized on the pyrrole nitrogen and *meso*-carbon atoms while the HOMO-1 (b_1) receives a major contribution from the α - and β -carbon. Therefore, to selectively red shift the B-band, an addition of π -conjugated groups at the *meso* position should be made. Similarly to selectively red-shift the Q-band, the addition of π -conjugated groups to the β position results in lowering of the energy.

Shown in Table 3 are calculated data for both D_{4h} and D_{2d} symmetry of ZnTPP and PdTPP. The D_{4h} molecule is planar whereas the D_{2d} structure is slightly saddled. In the theoretical calculations we are able to hold the geometry of the MTPP chromophore planar (a) to calculate only the percentage of the red shift that is attributed to electronic effects and eliminate that due to distortion. The experimental data include distortion effects (a*) from saddling of the porphyrin. It is known from X-ray crystallography data⁴⁷ that the MTPP ring of the metalated

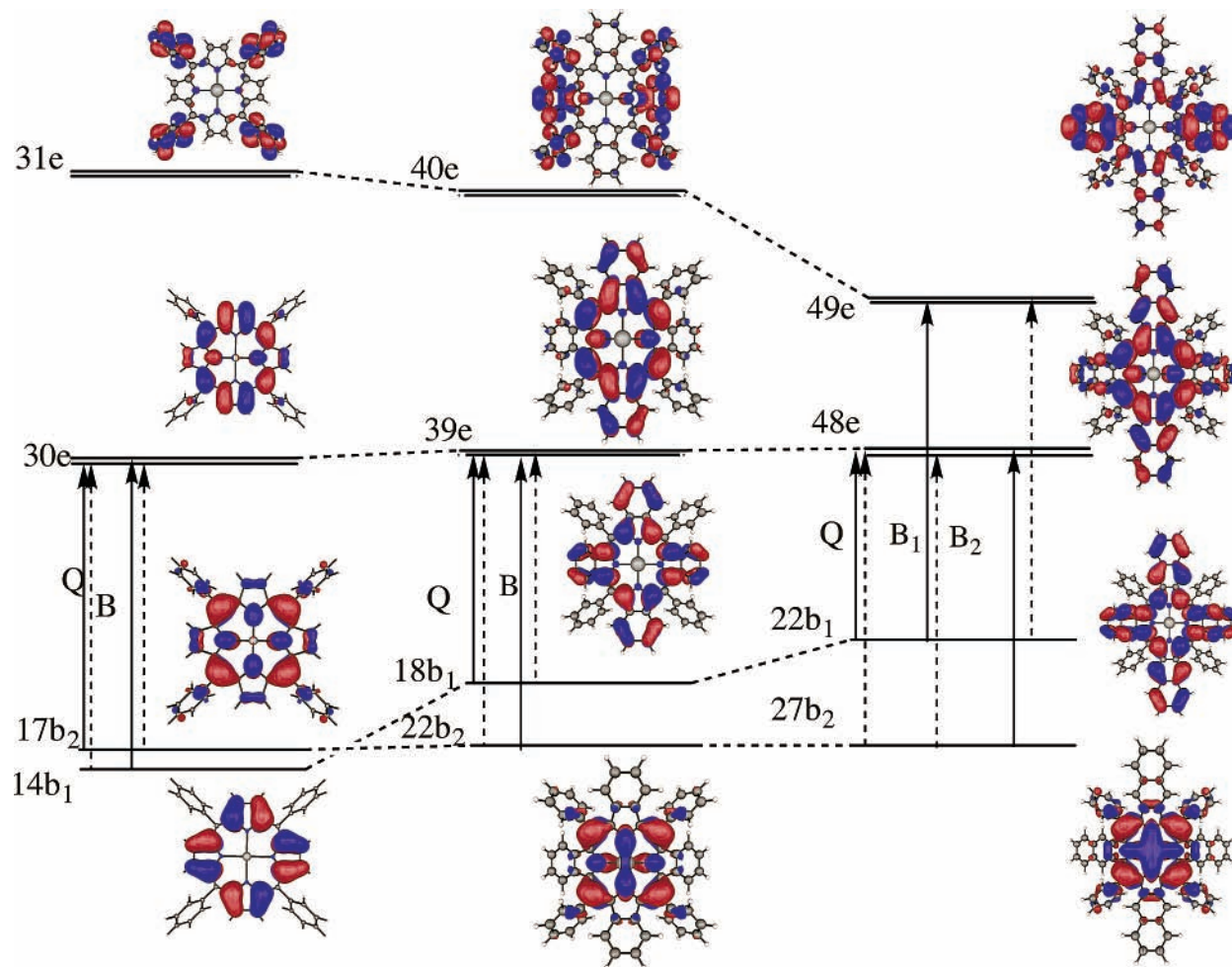


Figure 5. Molecular orbital diagrams for the Q- and B-transitions of zinc *meso*-tetraphenylporphyrin and its annulated derivatives. Solid and dotted arrows represent the major and minor contributions, respectively.

chromophore is fairly planar with a slight saddle formation. However, the phenyl groups are twisted out of the plane of the porphyrin by as much as 70–80°. The twisting and slight saddle formation is partly responsible for the red shift from metalloporphyrin (MP) to metalated *meso*-tetraphenylporphyrin (MTPP) as well as for the π -conjugation effects of the phenyl group to the porphyrin ring. The experimental data take this distortion into account when calculating the percentages due to each effect. Looking at the totals given in Table 4, the percentages are sometimes greater than 100%. For the experimental data this is due to slight saddle formation and also solvent effects. The theoretical data for the Q-band of ZnTPTNP and PdTPTNP also total to slightly more than 100%, suggesting that the substituents effects are not strictly additive.

Theoretical interpretations of the spectra of the parent compounds ZnP, ZnTBP, and ZnTTP have been presented previously.^{48,49} Detailed comparisons of the computed spectra with experiments have been given and will not be repeated here. The results for the parent systems, computed using the same level of theory as in the present work, are included in Table 3. They will serve as references for analyzing the cumulative effects of the benzo and phenyl groups on the absorption spectra. TDDFT results for the other porphyrins have not been reported. The average deviation between the computed excitation energies and the spectral maxima taken in benzene for the Q-band is about 0.2 eV. Slightly larger deviations are observed for the B-band. Figures 5 and 6 display principal molecular orbitals with major contributions to the excited state Q and B wave functions. For MTPP and MTPTBP, the origins of the Q- and

B-bands can be traced to the two highest occupied (HOMO and HOMO-1) and lowest unoccupied (LUMO and LUMO+1) MOs. Note that the HOMO and HOMO-1 are similar in energy in MTPP while they are well separated in MTPTBP (see Figures 5 and 6). However, these orbitals and the degenerate LUMOs are well separated from the rest of the occupied and virtual MOs. This type of MO arrangement provides the basis for the “four-orbital model” to interpret the Q- and B-bands.⁵⁰ In MTPP, the HOMO (b_2) coefficients are largely localized on the pyrrole nitrogen and *meso*-carbon atoms, while the HOMO-1 (b_1) receives a major contribution from the α - and β -carbons. Thus, tetrabenzo and tetranaphtho annulations significantly destabilize the HOMO-1 of MTPP but leave the energy of the HOMOs and LUMOs largely unchanged. The destabilization of the HOMO-1 in MTPTBP and MTPTNP removes the quasi-degeneracy of two highest occupied MOs found in MTPP. This, by itself, does *not* cause a serious breakdown in the four-orbital approximation. However, in MTPTNP, HOMO-1 and LUMO are *not* well separated from other occupied and virtual MOs. Apparently, the assumption that the degenerate LUMOs are well separated from the rest of the virtual MOs, which provides the basis for Gouterman’s four-orbital model, does not hold for MTPTNP. This type of MO arrangement (also found in the nonphenylated MTNP series) gives rise to an additional allowed (and nonallowed) transition in the B region. On the basis of their PPP calculations, Kuz’mitskii et al. have predicted the complication of the ZnTNP absorption spectrum in the B region due to the appearance of additional transitions.⁵¹ Our TDDFT calculations support their conclusions.

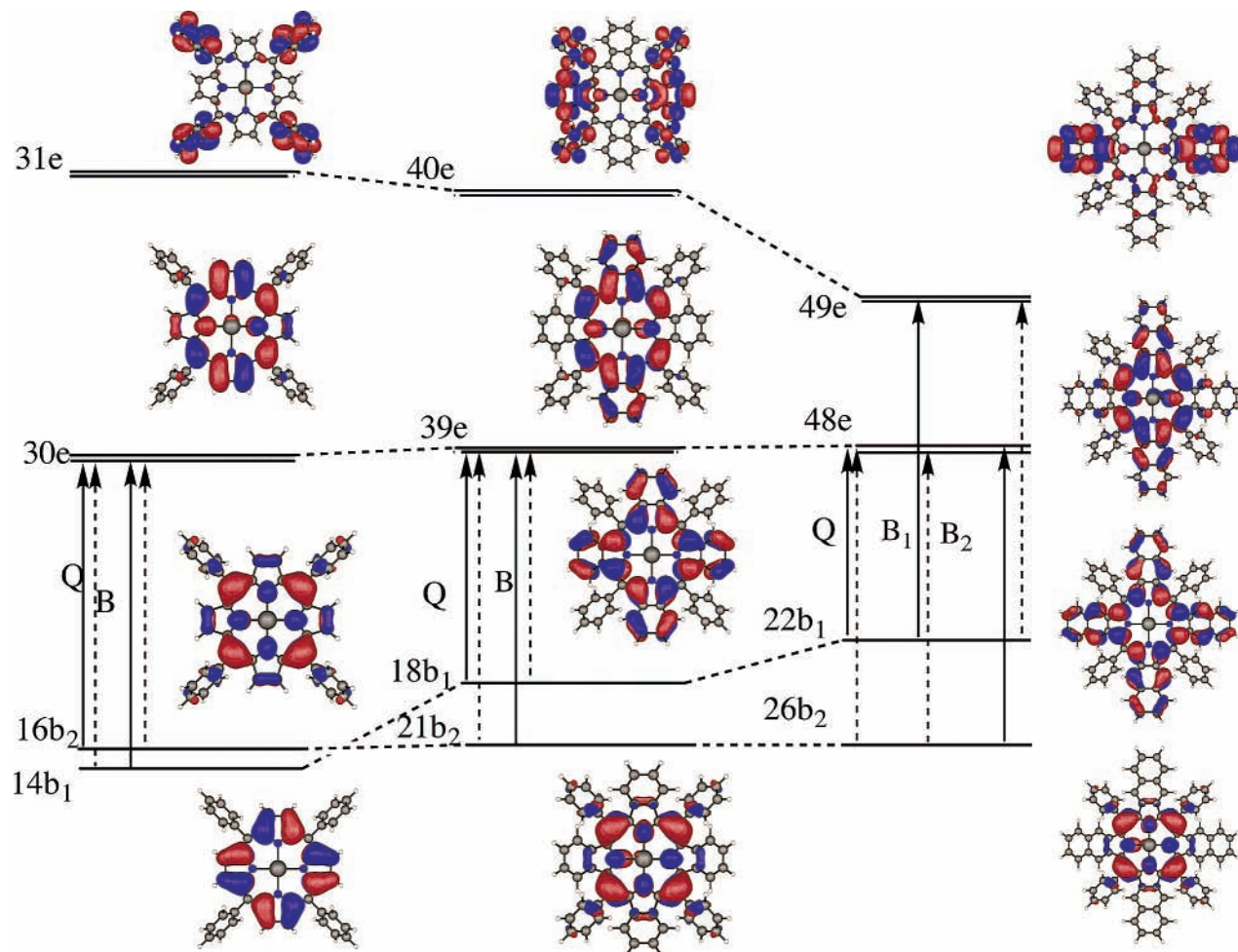


Figure 6. Molecular orbital diagrams for the Q- and B-transitions of palladium *meso*-tetraphenylporphyrin and its annulated derivatives. Solid and dotted arrows represent the major and minor contributions, respectively.

In unsubstituted metalloporphyrin (MP) and metalated *meso*-tetraphenylporphyrin (MTTP), the two main configurations, $a_{1u} \rightarrow e_g$ and $a_{2u} \rightarrow e_g$ and $b_2 \rightarrow e$ and $b_1 \rightarrow e$, respectively, are almost degenerate (to a lesser extent for MTTP), and their transition moments essentially cancel each other. The incomplete cancellation of transition moments for porphyrin derivatives was identified by Weiss et al.⁵² In the annulated porphyrins, the absence of quasi-degeneracy between HOMO and HOMO-1 leads to an increase in the intensity of the Q-band due to the minor contribution from the $b_2 \rightarrow e$ configuration. Thus, the origin of the increase in the intensity of the Q-band is connected to the reduction in b_1-e orbital energy gaps that can be attributed to the destabilization of the HOMO-1 of MTTP.

A red shift and a broadening in the triplet-excited state spectra were observed with benzo or naphtho annulation (Figure 4). For both the Pd and Zn series similar spectral changes were observed. The MTTP chromophores have very intense peaks directly to the red of the B-bands with only small absorptions to the red of the Q-bands. For MTPTBP we see a broader absorption from 400 to 600 nm that consists of two peaks. For MTPTNP the broadest absorption spectrum is found that contains several peaks. The origin of this broadening with annulation is not understood.

Effect of Metal. Comparing the ground state spectra of the Zn and Pd chromophores, we note that the bands in the Zn series are further red-shifted than for the Pd porphyrins. The B-band shift observed in pyridine and benzene (shown in parentheses) is about 0.09 (0.04) eV shift for MTTP, 0.17 (0.11) eV shift

for MTPTBP, and a 0.21 (0.11) eV shift for MTPTNP. For the Q-band the opposite is observed with a 0.18 (0.13) eV shift for MTTP, a 0.09 (0.07) eV shift for MTPTBP, and a 0.04 (0.05) eV shift for MTPTNP, in pyridine (benzene). Note that for the B-band a larger shift is observed in the MTPTNP macrocycle, whereas for the Q-band there is a larger shift for MTTP. Gas-phase TDDFT calculations reveal only modest effects on changing the central metal. Therefore, we can assume that the metal contributes differently in the annulated systems than in MTTP.

The triplet excited state spectra are similar for both Zn and Pd porphyrins. There is a small effect on the triplet excited state spectrum by the metal used. Comparing the data in Figure 4, we note that the shapes of the transient absorption spectra are similar for ZnTTP and PdTTP with a sharp peak around 475 nm and a small absorption at lower energies. For ZnTPTBP and PdTPTBP the spectra contain two larger absorptions in the region from 400 to 600 nm. For ZnTPTNP and PdTPTNP the spectra contain more different features. While both are broad, i.e., from 400 to 800 nm, there are several peaks that differ with metal. To better understand these features, calculations on the triplet excited states are being carried out.

Kinetic Changes. Effect of Extension of Porphyrin Ring. The effect of annulation on the kinetic properties for a series of porphyrins is varied. Comparing the quantum yields and lifetimes (Table 2), no clear trend is observed as a function of annulation, indicating a complex interaction of causes. Comparing the intersystem crossing quantum yields given in Table 2,

TABLE 5: Rate Constants of Singlet and Triplet State Relaxation

	ZnTPP	ZnTPTBP	ZnTPTNP	PdTPP	PdTPTBP	PdTPTNP
k_s (s ⁻¹)	3.7×10^8 ^a	1.5×10^9 ^b		5.0×10^{10} ^c		
k_f (s ⁻¹)	1.1×10^7	1.1×10^7		2.0×10^7		
k_{ISC} (s ⁻¹)	3.1×10^8	1.5×10^9		4.8×10^{10}		
k_{ICS} (s ⁻¹)	4.9×10^7	2.7×10^7		2.0×10^9		
k_T (s ⁻¹) ^d	2.7×10^2	6.0×10^3	2.3×10^3	9.1×10^5	5.1×10^3	1.7×10^4
k_p (s ⁻¹)	1.6×10^{-1}	6.0×10^{-2}	7.3×10^{-1}	3.8×10^2	8.8×10^2	1.4×10^3
k_{ICT} (s ⁻¹)	2.7×10^2	6.0×10^3	2.3×10^3	9.1×10^4	4.2×10^3	1.5×10^4

^a Measured in methylcyclohexane; *J. Chem. Soc., Faraday Trans. 1* **1980**, 76, 1978. ^b Measured in benzene; *J. Phys. Chem.* **1996**, 100, 17507. ^c Measured in methylcyclohexane; *J. Chem. Soc., Faraday Trans. 2* **1981**, 77, 1281. ^d Values from Table 2 (phosphorescence decay); $k_T = 1/\tau_T$.

TABLE 6: Calculated 6-31G(d) Energies of Triplet Excited State Levels^a

	ZnTPP	ZnTPTBP	ZnTPTNP	PdTPP	PdTPTBP	PdTPTNP
T ₁ (eV)	1.61	1.44	1.19	1.75	1.54	1.32
T ₂ (eV)	1.92	1.80	1.51	2.03	1.86	1.60
T ₃ (eV)	2.21	2.01	2.10	2.25	2.15	2.17
T ₄ (eV)	3.18	3.10	2.27	2.67	2.54	2.25
S ₁ (eV) ^b	2.30	2.05	1.82	2.40	2.14	1.90

^a T₁ energies are the computed adiabatic values while T_{1+n} are computed with the T₁ geometries. ^b Energies from calculated maximum of Q-band from Table 3.

it is interesting to note that for both metals we see a decrease in the triplet quantum yield for MTPTNP and an increase for MTPTBP relative to MTPP.

Listed in Table 5 are the calculated rates for decay from both the singlet (using published singlet state lifetimes of ZnTPP, PdTPP, and ZnTPTBP)^{39,42} and triplet excited state. Comparing the rate constants for decay from the singlet excited state (fluorescence (k_f), intersystem crossing (k_{ISC}), and internal conversion (k_{ICS})), we note that intersystem crossing is the predominant pathway of relaxation. We know that the intersystem crossing quantum yield of MTPTNP is smaller than these in the other chromophores, and we do not see a large increase in its fluorescence quantum yield, so we expect that internal conversion from the singlet state is more competitive for this chromophore. This might be expected solely on the basis of the singlet state energies (E_{S1} , given in Table 2). With extension of the π -system we observe a remarkable red shift of the ground state spectrum with a lowering of the singlet excited state energy, thus providing an easier pathway of relaxation. We hope to measure the singlet state lifetimes in the near future.

In an attempt to better understand the process of intersystem crossing from the singlet excited state to the triplet excited state, the triplet excited state levels were calculated using TDDFT and are shown in Table 6. Assuming that intersystem crossing is occurring exclusively from the lowest energy singlet state (S₁), comparing the triplet excited state levels with the first singlet excited state level (S₁), the data show that some of the energy levels overlap. Given in Table 6 are the S₁ energies and the various T₁ levels. For ZnTPP, ZnTPTBP, PdTPP, and PdTPTBP the energy of the S₁ state overlaps fairly well with the T₃ level with only small gaps in energy (<0.15 eV). For both ZnTPTNP and PdTPTNP there is a larger gap (0.31 and 0.30 eV, respectively) between S₁ with the T₂ level, and the T₃ state is much higher in energy and unattainable by the S₁ state. Therefore, the singlet–triplet coupling for ZnTPP, ZnTPTBP, PdTPP, and PdTPTBP is larger than for ZnTPTNP and PdTPTNP comparatively, and thus intersystem crossing is faster resulting in larger quantum yields.

In Table 5 a comparison is also made for the decay of the triplet excited state. For both metal series internal conversion from the triplet excited state is the predominant pathway for relaxation. For the Pd series there is a trend that the rate of phosphorescence decay (k_p) increases with annulation. This is

not the case for the Zn series. However, for the Zn series we observe an increase in internal conversion (k_{ICT}) from the triplet state as a function of increased annulation. We do not see this for the Pd series. Since no clear trend is observed, this indicates that no single process is dominating, but rather there is a complex interaction of several processes.

Effect of Metal. An effect of varying the central metal from Zn to Pd is observed in the kinetic parameters we measured. Pd is a heavier atom, so it influences the production of the triplet state, resulting in faster intersystem crossing through enhanced spin–orbit coupling. It has been reported⁵³ that an increase in spin–orbit coupling alters the photophysical processes in such a way that (a) an increase in phosphorescence quantum yield is observed, (b) an increase in the radiative rate constant of phosphorescence, (c) a decrease in fluorescence quantum yield, and (d) an increase in the rate constant of intersystem crossing. Comparing the data from Table 2 and Table 5, all of the above effects on the photophysical processes are met. For the Pd series relative to the Zn series there is an increase in the phosphorescence quantum yield, an increase in the radiative rate constant of phosphorescence is observed, and a decrease in the fluorescence quantum yield was determined. Comparing the limited data of intersystem crossing, we observe a large increase in the rate constant for PdTPP relative to ZnTPP. We assume that the same trend would be true for the annulated porphyrins solely on the basis of the heavy atom effect. Heavy atoms change spin–orbit coupling, with little relative change in energy levels and spectra of the annulated forms, giving an independent control of intersystem crossing.

Conclusions

The trends observed for Zn and Pd series of structurally related porphyrins provide the basis for understanding the photophysical properties inherent for these types of chromophores. Extension of the porphyrin ring leads to dramatic red shifts in the ground state spectra that are mainly due to increased conjugation effects with contributions from distortion. The red shifts observed for these annulated porphyrins can be traced to the destabilization of the HOMO-1 of the tetraphenylporphyrins. A red shift in the ground state spectra was observed when changing the central metal from Pd to Zn, thus indicating involvement of the metal in the optical transitions. The kinetic parameters of these chromophores are more de-

pendent on the central metal than on the extension of the π system. A significant heavy atom effect was observed in Pd porphyrins. Naphtho annulation did lead to a decreased overall intersystem crossing quantum yield in both the Zn and Pd porphyrins. This may be attributed to a difference in the number of favorable S_1-T_n channels, as predicted by the TDDFT calculations. Future directions of this research include modifications of the structure of the annulated porphyrin by adding various functional groups to the benzo and/or naphtho region for maintaining solubility in the absence of the *meso*-phenyl groups.

Acknowledgment. We are thankful for the support of this work by AFRL/ML Contracts F33615-99-C-5415 for D.G.M. and F33615-97-D-5403 for J.E.R., K.A.N., D.C.H., W.S., and K.M.G. The calculations were performed on computers at the Aeronautical Systems Center (ASC) Major Shared Resource Center (MSRC). The support provided by the ASC MSRC Service Center is greatly appreciated. We also thank Prof. Kirk Schanze at the University of Florida for the photoacoustic calorimetry data.

References and Notes

- (1) Milgrom, L. R. *The Colours of Life*; Oxford University Press: Oxford, 1997.
- (2) Kadish, K. M.; Smith, K. M.; Guillard, R. *The Porphyrin Handbook*; Academic Press: San Diego, 2000.
- (3) Ichimura, K.; Sakuragi, M.; Morii, H.; Yasuike, M.; Fukui, M.; Ohno, O. *Inorg. Chim. Acta* **1990**, *176*, 31.
- (4) Cheng, R.; Chen, Y.; Chung, C. *Heterocycles* **1992**, *34*, 1.
- (5) Cheng, R.; Chen, Y.; Wang, S. L.; Cheng, C. Y. *Polyhedron* **1993**, *12*, 1353.
- (6) Remy, D. E. *Tetrahedron Lett.* **1983**, *24*, 1451.
- (7) Vinogradov, S. A.; Wilson, D. F. *J. Chem. Soc., Perkin Trans. 2* **1995**, 103.
- (8) Finikova, O.; Cheprakov, A.; Beletskaya, I.; Vinogradov, S. A. *Chem. Commun.* **2001**, 261.
- (9) Ito, S.; Murashima, T.; Uno, H.; Ono, N. *Chem. Commun.* **1998**, 1661.
- (10) Ito, S.; Ochi, N.; Uno, H.; Murashima, T.; Ono, N. *Chem. Commun.* **2000**, 893.
- (11) Kopranev, V. N.; Dashkevich, S. N.; Lukyanets, E. Y. *Zh. Obshch. Khim.* **1981**, *51*, 2513. English translation: *J. Gen. Chem. USSR* **1981**, *51*, 2165.
- (12) Galanin, N. E.; Kudrik, E. V.; Shaposhnikov, G. P. *Zh. Obshch. Khim.* **1997**, *67*, 1393. English translation: *Russ. J. Gen. Chem.* **1997**, *67*, 1306.
- (13) Kopranev, V. N.; Vorotnikov, A. M.; Dashkevich, S. N.; Luk'yanets, E. A. *Zh. Obshch. Khim.* **1985**, *55*, 900. English translation: *J. Gen. Chem. USSR* **1985**, *55*, 803.
- (14) Antina, E. V.; Chernyshev, D. V.; V'yugin, A. I.; Kulinich, V. P.; Varannikov, V. P.; Krestov, G. A. *Zh. Fiz. Khim.* **1991**, *65*, 964. English translation: *Russ. J. Phys. Chem.* **1991**, *65*, 507.
- (15) Kuznetsova, N. A.; Gretsova, N. S.; Kalmykova, E. A.; Makarova, E. A.; Dashkevich, S. N.; Negrimovskii, V. M.; Kaliya, O. L.; Luk'yanets, E. A. *Zh. Obshch. Khim.* **2000**, *70*, 140. English translation: *Russ. J. Gen. Chem.* **2000**, *70*, 133.
- (16) Sapunov, V. V.; Solovev, K. N.; Kopranev, V. N.; Dashkevich, S. N. *Teor. Eksp. Khim.* **1991**, *1*, 105. English translation: *Theor. Exp. Chem.* **1991**, *1*, 99.
- (17) Ichimura, K.; Sakuragi, M.; Morii, H.; Yasuike, M.; Fukui, M.; Ohno, O. *Inorg. Chim. Acta* **1991**, *182*, 83.
- (18) Vinogradov, S. A.; Wilson, D. F. *Adv. Exp. Med. Biol.* **1997**, *411*, 597.
- (19) Rozhkov, V.; Khajehpour, M.; Vinogradov, S. *Inorg. Chem.*, in press.
- (20) Rogers, J. E.; Cooper, T. M.; Fleitz, P. A.; Glass, D. J.; McLean, D. G. *J. Phys. Chem. A* **2002**, *106*, 10108.
- (21) Lee, W. A.; Gratzel, M.; Kalyanasundaram, K. *Chem. Phys. Lett.* **1984**, *107*, 308.
- (22) Walters, K. A.; Schanze, K. S. *Spectrum* **1998**, *11* (2), 1.
- (23) Bauernschmitt, R.; Ahlrichs, R. *Chem. Phys. Lett.* **1996**, *256*, 454.
- (24) Casida, M.; Jamorski, C.; Casida, K. C.; Salahub, D. R. *J. Chem. Phys.* **1998**, *108*, 4439.
- (25) Stratmann, R. E.; Scuseria, G. E.; Frisch, M. J. *J. Chem. Phys.* **1998**, *109*, 8218.
- (26) Becke, A. D. *J. Chem. Phys.* **1993**, *98*, 5648.
- (27) Becke, A. D. *Phys. Rev. A* **1988**, *38*, 3098.
- (28) Lee, C.; Yang, W.; Parr, R. G. *Phys. Rev. B* **1988**, *37*, 785.
- (29) Ditchfield, R.; Hehre, W. J.; Pople, J. A. *J. Chem. Phys.* **1971**, *54*, 724.
- (30) Hehre, W. J.; Ditchfield, R.; Pople, J. A. *J. Chem. Phys.* **1972**, *56*, 2257.
- (31) Stevens, W. J.; Basch, H.; Krauss, M. *J. Chem. Phys.* **1984**, *81*, 6026.
- (32) Stevens, W. J.; Basch, H.; Krauss, M.; Jasien, P. *Can. J. Chem.* **1992**, *70*, 612.
- (33) Kohn, W.; Sham, L. J. *Phys. Rev. A* **1965**, *140*, 1133.
- (34) Frisch, M. J.; Trucks, G. W.; Schlegel, H. B.; Scuseria, G. E.; Robb, M. A.; Cheeseman, J. R.; Zakrzewski, V. G.; Montgomery, J. A.; Stratmann, R. E.; Burant, J. C.; Dapprich, S.; Millam, J. M.; Daniels, A. D.; Kudin, K. N.; Strain, M. C.; Farkas, O.; Tomasi, J.; Barone, V.; Cossi, M.; Cammi, R.; Mennucci, B.; Pomelli, C.; Adamo, C.; Clifford, S.; Ochterski, J.; Petersson, G. A.; Ayala, P. Y.; Cui, Q.; Morokuma, K.; Malick, D. K.; Rabuck, A. D.; Raghavachari, K.; Foresman, J. B.; Cioslowski, J.; Ortiz, J. V.; Stefanov, B. B.; Liu, G.; Liashenko, A.; Piskorz, P.; Komaromi, I.; Gomperts, R.; Martin, R. L.; Fox, D. J.; Keith, T.; Al-Laham, M. A.; Peng, C. Y.; Nanayakkara, A.; Gonzalez, C.; Challacombe, M.; Gill, P. M. W.; Johnson, B. G.; Chen, W.; Wong, M. W.; Andres, J. L.; Head-Gordon, M.; Replogle, E. S.; Pople, J. A. *Gaussian 98*, revision A.11; Gaussian, Inc.: Pittsburgh, PA, 1998.
- (35) Tsvirko, M. P.; Sapunov, V. V.; Solovev, K. N. *Opt. Spektrosk.* **1973**, *34*, 1094. English translation: *Opt. Spectrosc.* **1973**, *34*, 635.
- (36) Quimby, D. J.; Longo, F. R. *J. Am. Chem. Soc.* **1975**, *97*, 5111.
- (37) Vogler, A.; Rethwisch, B.; Kunkely, H.; Huttermann, J. *Angew. Chem., Int. Ed. Engl.* **1978**, *17*, 952.
- (38) Miller, J. R.; Dorough, G. D. *J. Am. Chem. Soc.* **1952**, *74*, 3977.
- (39) Harriman, A. *J. Chem. Soc., Faraday Trans. 1* **1980**, *76*, 1978.
- (40) Pekkari, L.; Linschitz, H. *J. Am. Chem. Soc.* **1960**, *82*, 2407.
- (41) Ono, N.; Ito, S.; Wu, C. H.; Chen, C. H.; Wen, T. C. *Chem. Phys.* **2000**, *262*, 467.
- (42) Chen, P.; Tomov, I. V.; Dvornikov, A. S.; Nakashima, M.; Roach, J. F.; Alabran, D. V.; Rentzepis, P. M. *J. Phys. Chem.* **1996**, *100*, 17507.
- (43) Harriman, A.; Porter, G.; Wilowska, A. *J. Chem. Soc., Faraday Trans. 2* **1983**, *27*, 807.
- (44) Gouterman, M. *The Porphyrins*; Academic Press: New York, 1978; Vol. III, pp 1-165.
- (45) (a) Medforth, C. J.; Berber, M. D.; Smith, K. M.; Shelnut, J. A. *Tetrahedron Lett.* **1990**, *31*, 3719. (b) Medforth, C. J.; Senge, M. O.; Smith, K. M.; Sparks, L. D.; Shelnut, J. A. *J. Am. Chem. Soc.* **1992**, *114*, 9859. (c) Shelnut, J. A.; Song, X.; Ma, J.; Jia, S.; Jentzen, W.; Medforth, C. J. *Chem. Soc. Rev.* **1998**, *27*, 31. (d) Chirvony, V. S.; Hoek, A.; Galievsky, V. A.; Sazanovich, I. V.; Schaafsma, T. J.; Holten, D. *J. Phys. Chem. B* **2000**, *104*, 9909. (e) Sazanovich, I. V.; Galievsky, V. A.; Hoek, A.; Schaafsma, T. J.; Malinovskii, V. L.; Holten, D.; Chirvony, V. S. *J. Phys. Chem. B* **2001**, *105*, 7818. (f) Parusel, A. B. J.; Wondimagegn, T.; Ghosh, A. *J. Am. Chem. Soc.* **2000**, *122*, 6371. (g) DiMagno, S. G.; Wertsching, A. K.; Ross, C. R. *J. Am. Chem. Soc.* **1995**, *117*, 8279. (h) Wertsching, A. K.; Koch, A. S.; DiMagno, S. G. *J. Am. Chem. Soc.* **2001**, *123*, 3932. (i) Fonda, H. N.; Gilbert, J. V.; Cormier, R. A.; Sprague, J. R.; Kamioka, K.; Connolly, J. S. *J. Phys. Chem.* **1993**, *97*, 7024. (j) Senge, M. O.; Kalisch, W. W. *Inorg. Chem.* **1997**, *36*, 6103. (k) Lash, T. D. *J. Porphyrins Phthalocyanines* **2001**, *5*, 267. (l) Nguyen, K. A.; Day, P. N.; Pachter, R.; Tretiak, S.; Chernyak, V.; Mukamel, S. *J. Phys. Chem. A* **2002**, *106*, 10285. (m) Ryeng, H.; Ghosh, A. *J. Am. Chem. Soc.* **2002**, *124*, 8099. (n) Haddad, R. E.; Gazeau, S.; Pecaut, J.; Marchon, J. C.; Medforth, C. J.; Shelnut, J. A. *J. Am. Chem. Soc.* **2003**, *125*, 1253.
- (46) Tsvirko, M. P.; Sapunov, V. V.; Solovev, K. N. *Opt. Spektrosk.* **1973**, *34*, 1094. English translation: *Opt. Spectrosc.* **1973**, *34*, 635.
- (47) Scheidt, W. R.; Mondal, J. U.; Eigenbrot, C. W.; Adler, A.; Radonovich, L. J.; Hoard, J. L. *Inorg. Chem.* **1986**, *25*, 795.
- (48) Nguyen, K. A.; Pachter, R. *J. Chem. Phys.* **2001**, *114*, 10757.
- (49) Nguyen, K. A.; Day, P. N.; Pachter, R.; Tretiak, S.; Chernyak, V.; Mukamel, S. *J. Phys. Chem. A* **2002**, *106*, 10757.
- (50) Gouterman, M. *J. Mol. Spectrosc.* **1961**, *6*, 138.
- (51) Kuz'mitskii, V. A.; Solov'ev, K. N.; Knyukshto, V. N.; Shushkevich, I. K.; Kopranev, V. N.; Vorotnikov, A. M. *Teor. Eksp. Khim.* **1983**, *19*, 655.
- (52) Weiss, C.; Kobayashi, H.; Gouterman, M. *J. Mol. Spectrosc.* **1965**, *16*, 415.
- (53) McGlynn, S. P.; Azumi, T.; Kinoshita, M. *Molecular Spectroscopy of the Triplet State*; Prentice Hall: Englewood Cliffs, NJ, 1969.